Kinetic and Processing Aspects of Polypropylene–Phenol Formaldehyde Compatibilizer Preparation: Theory and Practice

K. LARSEN BØRVE,[1] H. K. KOTLAR,[2] C.-G. GUSTAFSON[1]

[1] The Norwegian Institute of Science and Technology, Department of Machine Design and Materials Technology, N-7034 Trondheim, Norway

[2] Statoil Research Centre, N-7005 Trondheim, Norway

Received 14 July 1997; accepted 1 October 1998

ABSTRACT: This work deals with the kinetic and processing aspects of the synthesis of a polypropylene–phenol formaldehyde graft copolymer compatibilizer. This compatibilizer is suitable for blends or alloys of polypropylene and engineering polymers having aromatic residues or functionality complementary to hydroxyl. The compatibilizer is synthesized from thermoplastic phenol formaldehyde (PF) resins and functionalized polypropylene (f-PP) by reactive extrusion. The reaction between maleic anhydride- (PP-*g*-MAH) and glycidyl methacrylate-functionalized (PP-*g*-GMA) PP and PF resins followed the predicted models normally used for solvent systems. In a twin-screw extruder, this synthesis was generally best performed in a screw profile offering very intensive mixing and, in particular, with kneading elements located early in the reaction zone. The reaction between PP-*g*-MAH and PF was enhanced by applying vacuum venting to the system. For the PP-*g*-GMA and PF reaction, no such effect of a vacuum was observed. The conversion of GMA, with or without catalyst, was generally significantly higher than for the MAH system. © 2000 John Wiley & Sons, Inc. J Appl Polym Sci 75: 371–378, 2000

Key words: Polypropylene compatibilizers; Phenol Formaldehyde resins; Polypropylene blends; PP-g-Maleic anhydride; PP-g-glycidyl methacrylate; Reactive extrusion; Kinetical behavior

INTRODUCTION

In a earlier article, the synthesis of a polypropylene-*graft*-phenol formaldehyde copolymers was demonstrated.[1] For this synthesis, it was clearly shown that the component viscosity ratio had a significant effect on the conversion of the reactants. Component viscosity ratios of close to 1 were observed to give optimum reaction conditions. This is also according to earlier stated theories.[2,3]

The present study was aimed at understanding the kinetic aspects of such reactions in an extruder reactor. In particular, the effects of screw design, vacuum venting, and use of catalysts were investigated. Also, the reaction behavior of such reactions along an extruder screw was studied.

Kinetics of the Esterification Reaction of Maleic Anhydride (MAH) and Hydroxyl

The mathematical treatment of the kinetics of a particular chemical mechanism is given in stan-

Correspondence to: K. L. Børve, Borealis AS, Department of Polymer Development, Rønningen, N-3960 Stathelle, Norway.

Contract grant sponsors: Norwegian Research Council (NFR); Borealis AS, Bamble.

Journal of Applied Polymer Science, Vol. 75, 371–378 (2000)
 CCC 0021-8995/00/030371-08

dard reaction kinetics textbooks (e.g., Smith[4]). Details of the esterification reaction are not described in these textbooks and are, hence, included in this report. Maier[5] gave a similar detailed description of the reaction kinetics of MAH-grafted polyolefins and various lower alcohols.

Assuming a homogeneous reaction media, that the reaction occurs according to the functional groups present, and that no volatilization occurs, the equilibrium of esterification can be expressed as

$$\mathrm{ROH} + \mathrm{MAH} \underset{k_{-1,E}}{\overset{k_{1,E}}{\rightleftharpoons}} E \tag{1}$$

where ROH stands for alcohol; MAH, for cyclic anhydride; and E, for the ester formed.

The net rate of consumption of the MAH groups is given by the combination with alcohol plus the reverse esterification, the ester hydrolysis:

$$-\frac{dC_{\mathrm{MAH}}}{dt} = k_{1,E}C_{\mathrm{MAH}}C_{\mathrm{ROH}} - k_{-1,E}C_E \tag{2}$$

The concentration of various functional groups can be expressed in terms of only one functional group. Simplifying the further mathematical treatment by using only one variable leads to eq. (3):

$$C_{\mathrm{ROH}} = C^0_{\mathrm{ROH}} - (C^0_{\mathrm{MAH}} - C_{\mathrm{MAH}})$$

$$C_E = C^0_E + C^0_{\mathrm{MAH}} - C_{\mathrm{MAH}} \tag{3}$$

Introducing this to eq. (2) gives eq. (4):

$$\begin{aligned} -\frac{dC_{\mathrm{MAH}}}{dt} &= k_{1,E}C_{\mathrm{MAH}}(C^0_{\mathrm{ROH}} - C^0_{\mathrm{MAH}} + C_{\mathrm{MAH}}) \\ &\quad - k_{-1,E}(C^0_g + C^0_{\mathrm{MAH}} - C_{\mathrm{MAH}}) \\ &= -(k_{-1,E}C^0_{\mathrm{MAH}} + k_{-1,E}C^0_g) \\ &\quad + (k_{-1,E} + k_{1,E}C^0_{\mathrm{ROH}} - k_{1,E}C^0_{\mathrm{MAH}})C_{\mathrm{MAH}} + k_{1,E}C^2_{\mathrm{MAH}} \end{aligned} \tag{4}$$

Substituting of $k = k_{1,E}/k_{-1,E}$ leads to eq. (5) or the more simplified eq. (6):

$$\begin{aligned} -\frac{1}{k_{1,E}}\frac{dC_{\mathrm{MAH}}}{dt} &= -\frac{(C^0_{\mathrm{MAH}} + C^0_g)}{k} \\ &\quad + \left(\frac{1}{k} + C^0_{\mathrm{ROH}} - C^0_{\mathrm{MAH}}\right)C_{\mathrm{MAH}} + C^2_{\mathrm{MAH}} \end{aligned} \tag{5}$$

$$-\frac{1}{k_{1,E}}\frac{dC_{\mathrm{MAH}}}{dt} = C_1 + C_2C_{\mathrm{MAH}} + C^2_{\mathrm{MAH}} \tag{6}$$

where the constants of eq. (6) are

$$C_1 = -\frac{C^0_{\mathrm{MAH}} + C^0_g}{k} \tag{7}$$

$$C_2 = \frac{1}{k} + C^0_{\mathrm{ROH}} - C^0_{\mathrm{MAH}} \tag{8}$$

$$\frac{1}{C_3}\ln\left(\frac{2C_{\mathrm{MAH}} + C_2 - C_3}{2C_{\mathrm{MAH}} + C_2 + C_3}\cdot\frac{2C^0_{\mathrm{MAH}} + C_2 + C_3}{2C^0_{\mathrm{MAH}} + C_2 - C_3}\right) = -kt \tag{9}$$

Equation (6) can be solved analytically, using the criteria

$$C_{\mathrm{MAH}}(t = 0) = C^0_{\mathrm{MAH}}$$

where $C_3 = \sqrt{C_2^2 - 4C_1}$.

If the conversion is defined as

$$X_{\mathrm{MAH}} = \frac{C^0_{\mathrm{MAH}} - C_{\mathrm{MAH}}}{C^0_{\mathrm{MAH}}} \tag{10}$$

where C^0_{MAH} is defined as the level of conversion when no ester has been formed. Solving for C_{MAH} from eq. (9) gives

$$C_{\mathrm{MAH}} = \frac{1}{2}\left(\frac{(C_2 + C_3)e^{-C_3kt} + (C_3 - C_2)C_4}{C_4 - e^{-C_3kt}}\right) \tag{11}$$

where $C_4 = (2C^0_{\mathrm{MAH}} + C_2 + C_3)/(2C^0_{\mathrm{MAH}} + C_2 - C_3)$. At equilibrium, the net reaction rate is zero, and the equilibrium constant can be expressed as in eq. (12):

$$\begin{aligned} K_E &= \frac{C_{E,\mathrm{eq}}}{C_{A,\mathrm{eq}}C_{\mathrm{MAH,eq}}} \\ &= \frac{C^0_E + C^0_{\mathrm{MAH}} - C_{\mathrm{MAH,eq}}}{C_{A,\mathrm{eq}}(C^0_{\mathrm{MAH}} - (C^0_{\mathrm{MAH}} - C_{\mathrm{MAH,eq}})} \end{aligned} \tag{12}$$

Rearranging eq. (12) to isolate the equilibrium concentration of MAH yields

$$C_{\mathrm{MAH,eq}} = \frac{1}{2}\left((C^0_{\mathrm{MAH}} - C^0_{\mathrm{ROH}}) - \frac{1}{K_E} \pm \sqrt{\frac{(C^0_{\mathrm{ROH}} - C^0_{\mathrm{MAH}})^2}{+\frac{2(C^0_{\mathrm{MAH}} + C^0_{\mathrm{ROH}} + 2C^0_E)}{K_E} + \frac{1}{K^2_E}}}\right) \quad (13)$$

Kinetics of the Ring-opening Reaction of Glycidyl Methacrylate (GMA) and Hydroxyl

Assuming a homogeneous reaction medium, that the reaction between GMA and phenol formaldehyde (PF) occurs according to the functional groups present, and that no volatilization occurs, the ring-opening reaction of glycidyl ethers and phenols might be modeled as a spontaneous reaction:

$$\mathrm{ROH} + \mathrm{GMA} \xrightarrow{k_{\mathrm{AE}}} P \quad (14)$$

where ROH stands for the alcohol, and P, for the product formed. The net rate of consumption of the GMA groups is given by the reaction rate expression

$$-\frac{dC_{\mathrm{GMA}}}{dt} = k_{\mathrm{AE}} C_{\mathrm{GMA}} C_{\mathrm{ROH}} \quad (15)$$

The concentration of various functional groups can be expressed in terms of only one functional group, simplifying the further mathematical treatment by using only one variable:

$$C_{\mathrm{ROH}} = C^0_{\mathrm{ROH}} - (C^0_{\mathrm{GMA}} - C_{\mathrm{GMA}}) \quad (16)$$

Introducing this to eq. (15) gives

$$-\frac{dC_{\mathrm{GMA}}}{dt} = k_{\mathrm{AE}} C_{\mathrm{GMA}} (C^0_{\mathrm{ROH}} - C^0_{\mathrm{GMA}} + C_{\mathrm{GMA}}) \quad (17)$$

$$-\frac{dC_{\mathrm{GMA}}}{dt} = k_{\mathrm{AE}} (C^0_{\mathrm{ROH}} - C^0_{\mathrm{GMA}}) C_{\mathrm{GMA}} + k_{\mathrm{AE}} C^2_{\mathrm{GMA}} \quad (18)$$

Substituting $C_1 = C^0_{\mathrm{ROH}} - C^0_{\mathrm{GMA}}$ yields

$$-\frac{1}{k_{\mathrm{AE}}}\frac{dC_{\mathrm{GMA}}}{dt} = C_1 C_{\mathrm{GMA}} + C^2_{\mathrm{GMA}} \quad (19)$$

Equation (19) can be solved analytically, using the criteria

$$C_{\mathrm{GMA}}(t = 0) = C^0_{\mathrm{GMA}}$$

$$C_{\mathrm{GMA}} = \frac{(C^0_{\mathrm{ROH}} - C^0_{\mathrm{GMA}}) C^0_{\mathrm{GMA}}}{C^0_{\mathrm{ROH}} e^{(C^0_{\mathrm{ROH}} - C^0_{\mathrm{GMA}}) k_A t} - C^0_{\mathrm{GMA}}} \quad (20)$$

EXPERIMENTAL

Materials

One MAH-functionalized polypropylene (PP-*g*-MAH), one GMA-functionalized PP (PP-*g*-GMA), and one PF polymer provided the polymers. PP-*g*-MAH PB 3150 was supplied by Uniroyal Chemicals S.r.I. Latino Scalo, Italy. The measured MFI was 50 g/10 min (230°C/2.16 kg) and the amount of grafted MAH was 0.45 wt % (after vacuum drying).

PP-*g*-GMA was synthesized by free-radical grafting in the molten state, according to the procedures of Kotlar and Hansen[6] and Kotlar.[7,8] The measured MFI was 58 g/10 min (230°C/2.16 kg) and the amount of grafted GMA was 0.52 wt % (after vacuum drying).

The functionality contents of MAH and GMA were determined by FTIR[7,8] and titration methods. Functionality distributions of the functionalized polypropylenes (f-PPs) were determined by combined GPC and FTIR analyses. The results showed that the MAH and GMA functionalites were randomly grafted onto the PP phase and not fractions of high functionality mixed with ungrafted regions.

The thermoplastic PF polymer used in this study was an experimental grade from our own laboratory.[1] One grade with relatively high molecular weight was selected: KLB.017 (M_w 15,100, M_n 2830 g/mol).

Copolymers were prepared from a starting concentration of 80 wt % f-PP and 20 wt % PF. The f-PPs and the PF polymer were vacuum-dried at 100°C for 12 h before compounding to remove residual monomers and traces of water.

Synthesis

The kinetic study and predictions of the kinetic models for GMA and MAH f-PPs were conducted in a Brabender discontinuous mixer equipped with a 50-mL mixing chamber. The study of the effect of the processing conditions on the kinetics

for the formation of PP–PF graft copolymers was conducted in a 25-mm Clextral BC 21 intermeshing corotating twin-screw extruder (TSE) with an *L*/*D* of 44. f-PP and PF resin were fed into barrel 1, at a total throughput of 3 kg/h. The screw rotation speed was 200 rpm, and the barrel set temperature, 190–195°C. Average residence time at these conditions was 2.5 min. An inert atmosphere was used to reduce polymer degradation. The unreacted species and reaction by-products were vacuum vented from the extruder just after the second set of kneading elements and before the reaction product exited the extruder through a die. The extrudate was immediately quenched in a water bath and then pelletized.

The extruder screw profile was configured to allow good melting of the polymers followed by efficient mixing and high shear, high residence time in the reaction zone, and venting at the outlet of the extruder. In addition, four extruder screw setups with significantly different profiles were evaluated for the conversion of GMA along the extruder. Screw profiles 1 and 2 had an identical total number of mixing and kneading elements. However, the order of which they appeared along the screw was different. In screw profile 1, the 4 *L*/*D* neutral kneading block was located at 15–18 *D* (Fig. 5). For screw profile 2, the same block was located at 11–14 *D*. In screw profile 3, this neutral kneading block was replaced by medium-pitch conveying elements. In addition, the 4 *L*/*D* gear-mixing elements between 19 and 23 *D* were replaced by conveying elements. For screw profile 4, compared to screw profile 3, the neutral kneading discs and the reversible element at 9–11 *D* were replaced by small-pitch conveying elements. The extruder was equipped with a K'tron loss-in-weight feeding system for accurate feeding of the raw materials.

The reactivity comparison of MAH and GMA f-PP in a TSE was performed by repeated extrusion: After one cycle, the extruder strand was immediately quenched in ice-water, followed by pelletizing and a new extrusion cycle. The extrusion conditions were identical for each run, and samples were taken after each run for further analysis. The PP-*g*-MAH and PP-*g*-GMA grades involved contained the same level of functionality by mole.

Characterization

The reactants were determined by rheology, chromatography (GPC), spectroscopy (FTIR and NMR), and titration techniques for evaluation of the molecular structure and functionality. A systematic characterization of the blends was undertaken by thorough selective extraction followed by sample preparation and spectroscopic analysis. IR analysis was performed on a Perkin–Elmer 1725× FTIR instrument using transillumination, ATR total reflection, or reflection techniques.

The extraction method and solvent were adapted to this specific polymer system, and according to a solubility test on neat polymers, acetone was a selective solvent for PF polymers. Sufficient extraction time was 48 h on pellets followed by 48 h on film. The film was then repressed for FTIR analysis. Both extracted and nonextracted samples were analyzed. Materials (film) were predried before FTIR analysis at 100°C for 2 h. Films used in this study were sufficiently thin to be within an absorbance range where the Beer–Lambert law is obeyed (<0.6 absorbance units). Polymer films were made using a Pasadena hydraulic press and a distance frame of 0.1 mm.

For quantitative analysis of the amount of reacted PF polymer, data were obtained the FTIR spectrum of extracted samples, using the peak height ratio of the C═C peak (ring stretch) at 1610 cm^{-1} to that for the C—H peak (bend) at 973 cm^{-1}, and measured by the corresponding peak height ratio of the C═C peak (ring stretch) at 1641 cm^{-1} to that for the C—H peak (bend) at 899 cm^{-1}. These ratios were used as a measure for the relative content of PF in the graft copolymer. Calibration for routine FTIR determination of the absolute content of PF was obtained from a corresponding analysis of nonextracted samples. Since the PF is a rather high molecular weight species, the content of PF in the samples prior to extraction was assumed to be equal to the feeding content.

^{1}H-NMR and ^{13}C-NMR spectroscopy for characterization of the synthesized PF resins was conducted on a Bruker 500-MHz instrument. Samples were analyzed using a Bohlin CSM rheometer equipped with 25-mm parallel plates and a 1-mm gap setting. The rheometer was modified to reduce polymer degradation during analysis.

RESULTS AND DISCUSSION

Viscosities of Component Polymers

The melt viscosity as a function of the shear rate for PP-*g*-MAH, PP-*g*-GMA, and PF are shown in

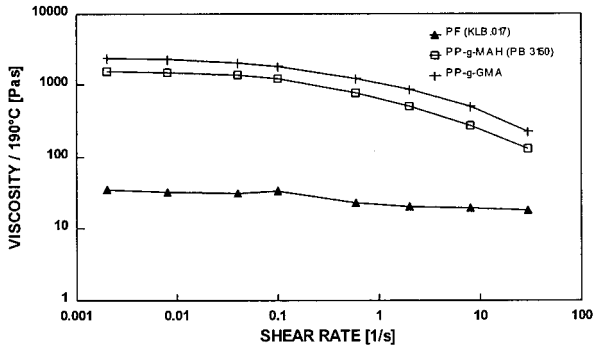

Figure 1 Viscosity of PP-*g*-MAH, PP-*g*-GMA, and PF as a function of shear rate at 190°C.

Figure 1. Since the measuring temperature was the same as the extrusion temperature, 190°C, the measured viscosity ratios indicate the ratio that dominated under the processing conditions. Typical shear rates during reactive extrusion will be 10^2–10^3 s^{-1}.[9] This value is assumed to best describe the average shear rate for a TSE equipped with various conveying, neutral kneading blocks, and gear-mixing elements. For the discontinuous Brabender mixer, shear rate is assumed to be in the lower range of this shear rate interval and perhaps below 10^2 s^{-1}. The effect of shear rate on the viscosity is much more noticeable for the higher molecular weight PP-*g*-MAH and PP-*g*-GMA than for the low molecular weight PF polymer. The PF polymer almost shows a Newtonian behavior. At shear rates typical for TSEs, the viscosity ratio between f-PP and PF approaches 1. For the Brabender mixer, the viscosity ratio is more likely to be between 1 and 5.

Synthesis of PP–PF in Discontinuous Mixer

PP–PF graft copolymers were synthesized by reaction in the molten stage using a Brabender discontinuous mixer. The PF contents in the formed PP–PF graft copolymers (PP-*g*-PF) were determined using selective extraction to remove unreacted PF, followed by FTIR. The efficiency of the extraction was checked by a control sample based on unmodified PP and 10 wt % PF. The extraction method removed all the PF polymer, as determined by FTIR.

The reaction between MAH f-PP and the PF polymer is shown in Figure 2. Starting concentrations were 80 wt % PP-*g*-MAH and 20 wt % PF, and the reaction temperature was 190°C. The PF polymer was introduced into the mixer after the f-PP had melted. In the figure, experimental data are shown for this system with and without a vacuum. The conversion of MAH was rather fast at this temperature, and for the system without a vacuum, a conversion plateau was reached after about 3 min of reaction. About 13% of the MAH was converted. When a vacuum was applied, somewhat different behavior was observed. The MAH conversion was generally higher, and a sim-

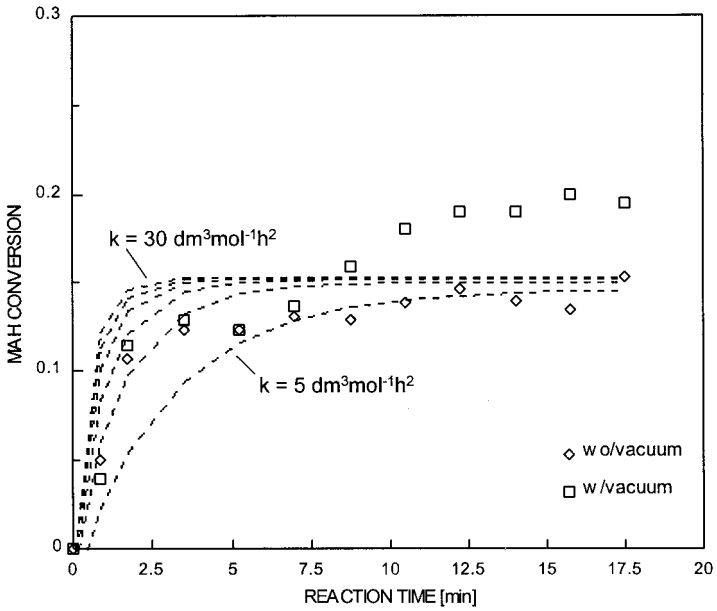

Figure 2 MAH conversion as a function of reaction time. Comparison of (data points) experimental and (– – –) theoretical data.

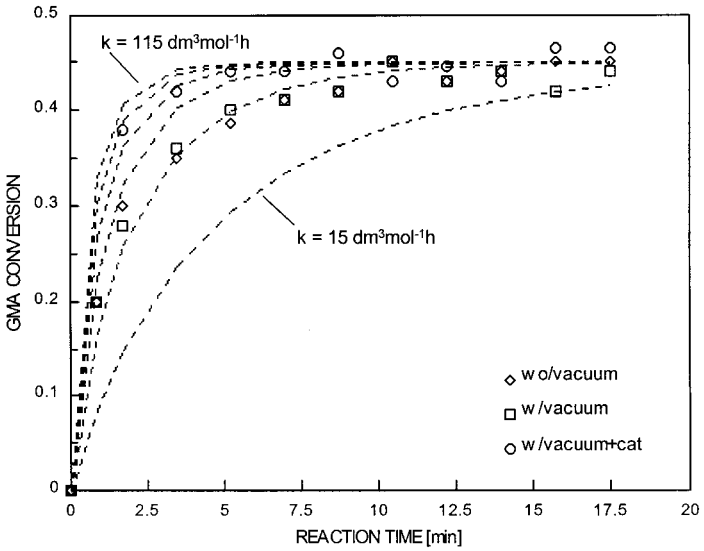

Figure 3 GMA conversion as a function of reaction time. Comparison of (data points) experimental and (– – –) theoretical data.

ilar plateau was observed at a higher reaction time: 15 min. More than 20% conversion was obtained. These observations are also known from earlier data.[10,11]

Curves from the kinetic model based on eq. (11) are added to the figure. Those six curves, presented in Figure 2, are based on various reaction rate constants, k, from 5 to 30 $dm^3\ mol^{-1}\ h^2$ with steps of 5. The correlation to the experimental data for $k = 10\ dm^3 mol^{-1}\ h^2$ was relatively good for the system without a vacuum. When a vacuum was applied, significant deviation from the model was observed. This deviation may come from more complex reactions, most likely from the reaction of the remaining carboxylic group on MAH. The first step (i) of the reaction of hydroxyls with MAH opens the ring:

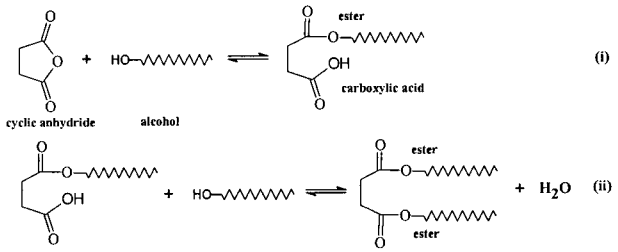

No water or reaction by-products are being generated in this step. In the second step (ii), the reaction proceeds like a normal esterification reaction, and water is generated. Both reaction steps are equilibrium reactions, and vacuum venting may move the second reaction step toward the product side.

The reaction between GMA f-PP and the PF polymer is shown in Figure 3. Starting concentrations were 80 wt % PP-*g*-GMA and 20 wt % PF, and the reaction temp-erature was 190°C, similar to PP-*g*-MAH and PF. Experimental data and modeling data are presented in the figure for systems with and without a vacuum and with a vacuum and a catalyst. The conversion of GMA was even faster than for MAH. Again, a conversion plateau was reached after about 3 min of the reaction. About 45 % of the GMA was reacted. No effect of the vacuum was observed in this case.

A base-catalyzed (KOH) reaction between PF and PP-*g*-GMA is also shown in Figure 3. In this case, the upper conversion plateau was obtained sooner, but the final conversion level was about the same as for the uncatalyzed reactions.

Six curves describing the kinetic model based on eq. (20) were added to the figure. Those six curves are based on reaction rate constants, k, ranging from 15 to 115 $dm^3\ mol^{-1}\ h$ with steps of 20. For the uncatalyzed reactions, the correlation to the experimental data was good for $k = 35\ dm^3\ mol^{-1}\ h$. Similarly, for the base-catalyzed reaction, a reaction rate constant of 75–85 $dm^3\ mol^{-1}\ h$ was achieved. Again, the correlation was fairly good.

For both the PP-*g*-MAH and the PP-*g*-GMA systems, the correlation between the experimental and the predicted models is fairly good. These

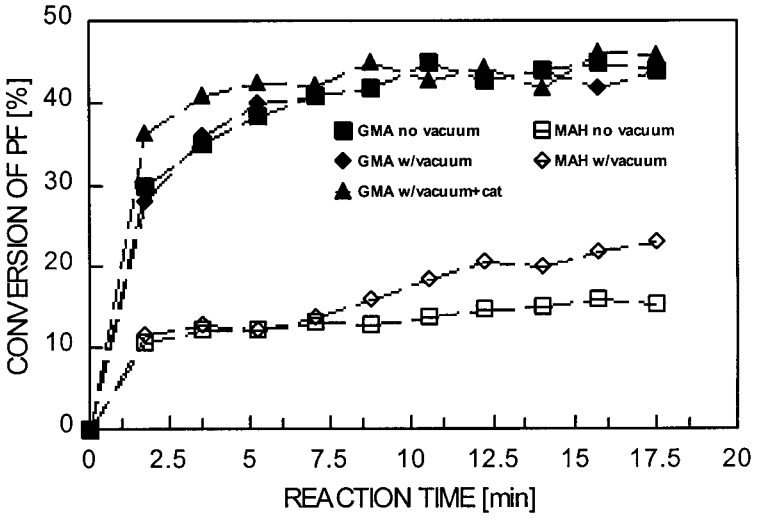

Figure 4 Conversion of PF–OH by repeated extrusion in TSE.

kinetic models are normally restricted to solvent-based reaction systems, offering significantly higher diffusion rates. In this present case, the necessary mobility of the molecules is assumed to be provided by the intensive mixing of the molten polymers.

Synthesis of PP–PF in Twin-screw Extruder

Synthesis of PP–PF graft copolymers was conducted in a TSE, and the kinetic behavior was studied using repeated extrusion. The same systems as studied in the Brabender mixer were studied by repeated extrusion: The extruder strand was quenched immediately after the die, pelletized, and extruded again. Samples for analysis were taken after each run. The conversion of PF as a function of reaction time for the MAH and GMA systems is presented in Figure 4. Almost the same reaction rates and upper conversion levels were obtained as for the discontinuous mixer. It is, however, interesting to note that the upper conversion plateaus were more or less reached after one extrusion. Significantly increasing the reaction time from longer extruders or by other means is not beneficial for these types of reactions. About 46 and 21% conversions of PF were achieved for PP-*g*-GMA and PP-*g*-MAH (with a vacuum), respectively.

Effect of Extruder Screw Profile

The effect of screw profiles on the conversion of GMA was studied from four different screw- profiles. Samples were taken from each barrel segment for every 4 *L*/*D* and immediately quenched in dry ice. The samples were then analyzed for conversion of GMA according to the established procedure.

The studied screw profiles and corresponding conversions of GMA are shown in Figure 5. Screw profile 2 was the most efficient screw profile for the overall conversion of GMA groups. More than 45 % conversion was observed. For this screw profile, the conversion was significantly higher at all sampling points on the extruder. Screw profile 1 was found to be the second most efficient one. A final conversion of about 33% was obtained. In screw profiles 1 and 2, no conversion was observed after 28 *L*/*D*. At this point, a plateau was reached. A conclusion from screw profiles 1 and 2 could be that kneading blocks should be installed closer to the feeding zone to enhance the conversion of such reactants.

For screw profiles 3 and 4, somewhat different behavior was observed. The conversion increased continuously along the screw length. For screw profile 3, the resulting conversion was close to that for number 1. Screw profile 4 was the least efficient and only about 20 % conversion was observed, less than one-half of that of screw profile 2.

CONCLUSIONS

PP–PF graft copolymers from thermoplastic PF resins and f-PP were synthesized by reactive extrusion. The reaction between PP-*g*-MAH and PP-

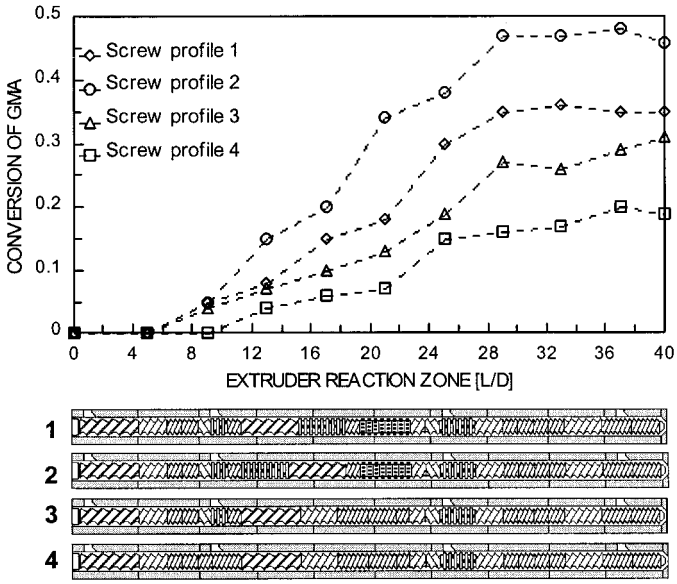

Figure 5 Conversion of PP-*g*-GMA as a function of extruder screw length for various screw profiles.

g-GMA and PF resins followed the predicted models normally restricted to solvent systems. In a TSE, this synthesis was generally best performed in a screw profile offering very intensive mixing and, in particular, with kneading elements located early in the reaction zone. Vacuum venting enhanced the conversion of PP-*g*-MAH. For the PP-*g*-GMA and PF reaction, no such effect of a vacuum was observed. The conversion of GMA, with or without a catalyst, was generally significantly higher than for the MAH system.

NOMENCLATURE

PP	polypropylene
PF	phenol formaldehyde resin
f-PP	functionalized PP
MAH	maleic anhydride
GMA	glycidyl methacrylate
PP-*g*-MAH	MAH-grafted PP
PP-*g*-GMA	GMA-grafted PP
FTIR	Fourier-transform IR spectroscopy

This work was part of a Ph.D. thesis and could not have been performed without the help of a number of people at Borealis AS and The Norwegian Institute of Science and Technology, Department of Machine Design and Materials Technology. This work was financed by the Norwegian Research Council (NFR) and Borealis AS, Bamble.

REFERENCES

1. Børve, K. L.; Kotlar, H. K., submitted for publication in Polymer.
2. Baker, W.; Liu, N. C. In Proceedings on Advances in Additives and Modifiers for Polymer Blends, Miami Beach, 1992.
3. Sammler, R. L.; Dion, R. P.; Carriere, C. J.; Cohen, A. Rheol Acta, in press.
4. Smith, J. M. Chemical Engineering Kinetics; McGraw-Hill: New York, 1981.
5. Maier, C. Ph.D. thesis, EAHP, Strasbourg, 1993.
6. Kotlar, H. K.; Hansen, P. M. PCT Patent Appl. WO 94/13 719 (to Borealis AS).
7. Kotlar, H. K. In Proceedings on Advances in Additives and Modifiers for Polymers and Blends, Clearwater Beach, FL, 1994.
8. Kotlar, H. K. In SPE, Tech Papers, ANTEC93, 1993; pp 1240–1248.
9. Eisele, U. Introduction of Polymer Physics; Springer-Verlag: New York, 1990.
10. Kotlar, H. K.; Børve, K. L. SPE, Tech Papers #1203/95, ANTEC95, 1995; p 1843.
11. Børve, K. L.; Kotlar, H. K.; Gustafson, C.-G., submitted for publication in J Appl Polym Sci.